THE JOURNAL OF PHYSICAL CHEMISTRY Letters

Letter

pubs.acs.org/JPCL

Recombination in Organic Bulk Heterojunction Solar Cells: Small Dependence of Interfacial Charge Transfer Kinetics on Fullerene Affinity

Antonio Guerrero,[†] Luis F. Marchesi,[†,‡] Pablo P. Boix,[†] Juan Bisquert,*[,†] and Germa Garcia-Belmonte*[,†]

[†]Photovoltaic and Optoelectronic Devices Group, Departament de Física, Universitat Jaume I, ES-12071 Castelló, Spain

[‡]Laboratório Interdisciplinar de Eletroquímica e Cerâmica (LIEC) Universidade Federal de São Carlos, São Carlos, Brazil

Supporting Information

ABSTRACT: We investigate the causes for obtaining higher open-circuit voltage in solar cells that use a fullerene with a smaller electron affinity. Using impedance spectroscopy technique, we show that the change of fullerene LUMO energy has very little influence on the kinetic rate of charge transfer across the interface. In terms of the Marcus theory, large reorganization energy values govern the recombination kinetic rate, which is only slightly dependent on the fullerene LUMO energy, and also depends weakly on the energy location of recombining carriers within the broad density of states. Since the recombination rate is very similar in the different devices, we conclude that the larger open-circuit voltage is due to the larger donor HOMO/acceptor LUMO offset.

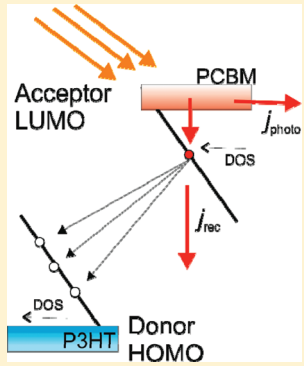

SECTION: Energy Conversion and Storage; Energy and Charge Transport

One of the current strategies for improving the power conversion efficiencies (PCEs) of solution-processed organic solar cells is the substitution of [6,6]-phenyl-C_{61}-butyric acid methyl ester ($PC_{60}BM$) as acceptor molecules by fullerene derivatives containing more side chains. It has been shown that electron acceptors with lower affinity give rise to enhanced open-circuit voltage V_{oc} because of the larger energy offset achievable, between the acceptor lowest unoccupied molecular orbital (LUMO) and the donor highest occupied molecular orbital (HOMO). Bis$PC_{60}BM$, a bisadduct analogue to $PC_{60}BM$, was shown to improve V_{oc} (0.73 V) with respect to that achieved with poly(3-hexylthiophene (P3HT):$PC_{60}BM$ systems, without a loss in photocurrent.[1] Similarly, trimetallic nitride endohedral fullerenes enhanced V_{oc} in 0.28 V.[2] More recently, indene-C_{60} bisadduct (ICBA)[3,4] and di(4-methylphenyl)methano-C_{60} bisadduct[5] have been proposed as acceptor candidates to achieve V_{oc} values higher than 0.8 V when P3HT is used as the donor polymer. The case of C_{60} derivatives blended with low-bandgap polymers has also been reported.[6] In all these cases, the enhancement in open-circuit voltage is attributed to a lower energy loss caused by the larger donor/acceptor unoccupied molecular orbital offset.

Improving the total solar cell internal interface gap (between the donor and acceptor) is not a sufficient condition to obtain higher voltage, V_F, which ultimately depends on the separation of Fermi levels as[7,8]

$$qV_F = E_{Fn} - E_{Fp} \quad (1)$$

Here q is the elementary charge. This last condition, in turn, depends on the ability of the blend to maintain a high concentration of separate electron and hole carriers, which is governed by recombination kinetics,[7] i.e., the rate of transfer of electrons in the acceptor material toward a hole in the donor material.

Previous work showed that the enhancement in open-circuit voltage in the case of 4,40-dihexyloxydiphenylmethano[60]-fullerene (DPM_6)[9] blended with P3HT is related to the combined effect of recombination reduction and intermediate density-of-state (DOS) occupancy. Whereas DPM_6 exhibits a full occupation of an electronic band, the electronic occupancy is restricted to lower-laying DOS states in the case of $PC_{60}BM$-based devices, despite exhibiting similar cyclic voltammetry reduction potentials.[9] It is then of crucial interest to distinguish the influence on the V_{oc} of materials energetics (HOMO and LUMO positions, and more featured state distributions entering the effective bandgap) on one hand, from the kinetics of charge carrier recombination on the other. This knowledge will allow for a more efficient donor/acceptor blend design, to consequently improve photovoltaic performance.

In this paper we compare the charge carrier recombination kinetics of bulk-heterojunction solar cells comprising different acceptors fullerenes, namely, ICBA, $PC_{60}BM$, and $PC_{70}BM$, using impedance methods under illumination. Several techni-

Received: April 1, 2012
Accepted: May 4, 2012
Published: May 4, 2012

   dx.doi.org/10.1021/jz3003958 | J. Phys. Chem. Lett. 2012, 3, 1386–1392

ques have been proposed to extract carrier recombination kinetics in organic solar cells. A family of techniques combine pulsed illumination and applied bias changes to collect photogenerated charges and derive transport and recombination parameters. Among these techniques, one can find photoinduced charge extraction in linearly increasing voltage (photo-CELIV),[10] integral mode time-of-flight,[11] and dark current injection.[12] These methods use bias voltage sweeps much larger than 1 V, and are characterized by the fact that photovoltaic devices do not operate under continuous irradiation. Since large biases are applied, current transient decays hardly exhibit exponential responses, and the derived lifetime (or recombination coefficient) is time-dependent. By means of such techniques, it is only feasible to determine an "effective" lifetime.[10] There exists another set of techniques that measure a transient response induced by a pulse of light that perturbs a steady state. Transient absorption spectroscopy[13] (TAS) is an optical measuring approach that monitors changes in optical density after photogeneration to extract the decay kinetics of excess carriers. A related method is based on modulated photoinduced absorption.[14] Similarly, transient photovoltage[15] (TPV) and photocurrent (TPC) allow for parameter extraction (lifetime and photoinduced carrier density) in conditions of continuous irradiation and small-amplitude perturbation. In addition to transient techniques, frequency-modulated methods (impedance spectroscopy (IS))[16] also fulfill the condition of applying a small-amplitude perturbation on a given steady state. Hence convergence of different parameter extraction methods is a crucial test for elucidating the validity of the measuring approach. TAS and TPV is known to give similar kinetic values.[15] Noticeably, differences of 1 order of magnitude between recombination coefficient extracted from photo-CELIV and TPV techniques have been reported for organic photovoltaic solar cells.[17] Such discrepancy has been attributed to the great difference in device operation between small-amplitude perturbation of continuous irradiation (TPV) and short intense light pulse out of steady state by applying a large voltage ramp (photo-CELIV). IS measurements have been reported to give recombination kinetics parameters similar to those extracted from analysis of TPV signals.[18]

As expected from lower electron affinity values, ICBA-based solar cells analyzed here exhibit higher photovoltage than devices made from PCBM, without a significant loss in photocurrent. We report the important finding that the recombination coefficient k is only *slightly dependent* on the fullerene LUMO energy, and always lies within the range of $k \approx 10^{-12}$ cm^3 s^{-1}. In addition, the situation of recombining carriers in the energy axis also has a minor influence on the value of the recombination coefficient. We finally conclude that V_{oc} enhancement is exclusively caused by the larger donor HOMO/acceptor LUMO offset, because the carrier recombination process appears to be highly independent of the fullerene energetics, even though the LUMO is heavily displaced, with respect to the polymer energy levels, in the different fullerenes. This is an unexpected finding, as it is usually thought that larger energy difference between donor and acceptor states increases the "driving force" for interfacial charge transfer, which should be reflected in higher value of the kinetic constant.

Solar cells of structure indium tin oxide (ITO)/poly(3,4-ethylenedioxythiophene):poly(styrene sulfonic acid) (PEDOT:PSS)/P3HT:fullerene/Ca/Ag, were prepared as described in the Experimental Section. As mentioned, three different fullerene acceptors have been tested to check the effect of the acceptor LUMO level shift on the overall recombination kinetics, and open-circuit voltage.

An example of the measured current-density voltage $j-V$ characteristics under simulated AM1.5G illumination (1000 W m^{-2}) of P3HT:fullerene solar cells is plotted in Figure 1. We

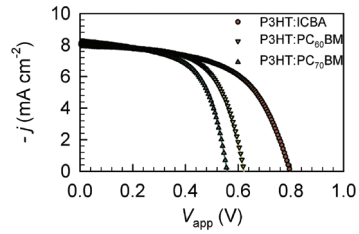

Figure 1. Current density–voltage characteristics of typical ITO/PEDOT:PSS/P3HT:fullerene/Ca/Ag devices, using ICBA, $PC_{60}BM$, and $PC_{70}BM$ as acceptors.

systematically observed that V_{oc} at 1 sun illumination results higher for cells processed with ICBA than that achieved when PCBM acceptors are used (see Table 1). Such difference attains values approximately equal to $\Delta V_{oc} \approx 0.2$ V, in good agreement with the less negative LUMO level position of the ICBA molecule. Cyclic voltammetry analysis of PCBM and ICBA molecules reveals a negative shift in the reduction peak of 0.17 V caused by the molecular LUMO position (−3.74 eV) compared to $PC_{60}BM$ (−3.91 eV).[3] Open-circuit voltage offset is then in good agreement with the experimentally observed correlation between the donor HOMO and acceptor LUMO difference (internal interface gap of the blend), and V_{oc} as $qV_{oc} \propto E_{LUMO}(A) - E_{HOMO}(D)$.[19] On the other hand, it is observed that short-circuit current attains similar values for all three kind of cells. It is widely agreed that internal morphology is a central factor governing cell operation, therefore structural similarity is a prerequisite to extract meaningful conclusions about the carrier recombination process. Figure 1 is interpreted in terms of a rather similar internal morphology that gives rise to comparable photocurrents.

To separate the influence of the charge carrier recombination process on the achievable V_{oc} from the aforementioned effect of the acceptor LUMO level energetics, we performed a series of impedance measurements in P3HT:fullerene BHJ solar cells, exhibiting power-conversion efficiency within the range of 2.7–3.7%, by varying the irradiation intensity in open-circuit conditions and applying a bias voltage V_F that equals V_{oc}.[16] As explained in eq 1, the applied voltage corresponds then to the splitting of the separated charge Fermi levels.

The extraction of resistive (R_{rec} recombination resistance) and capacitive (C_μ chemical capacitance) parameters from impedance measurements was explained in previous papers.[16,20] We show in Figure 2 the variation of R_{rec} and C_μ as a function of voltage. At low voltages, the measured capacitance responds to a dielectric mechanism. It is originated by the modulation of the depletion zone built up at the cathode contact, which collapses to the geometrical capacitance near zero voltage, as has been shown in our previous work.[20] By measuring the dark capacitance response in reverse and low forward voltages, one can extract the polymer doping level that is originated by structural and chemical defects made up during device preparation. Polymer doping produces a hole background

dx.doi.org/10.1021/jz3003958 | J. Phys. Chem. Lett. 2012, 3, 1386–1392

Table 1. Photovoltaic Parameters and Parameters Extracted from Impedance Spectroscopy Analysis of P3HT:Fullerene Solar Cells[a]

	j_{sc} (mA cm^{-2})	V_{oc} (V)	FF	PCE (%)	α	β	2α	p_0 (10^{15}cm^{-3})
P3HT:$PC_{60}BM$	8.05	0.62	0.62	3.1	0.34	0.64	0.68	3.65
P3HT:$PC_{70}BM$	8.36	0.56	0.59	2.7	0.37	0.73	0.74	9.61
P3HT:ICBA	8.14	0.80	0.57	3.7	0.38	0.74	0.75	30.2

[a]Polymer p-doping produces a hole background density p_0.

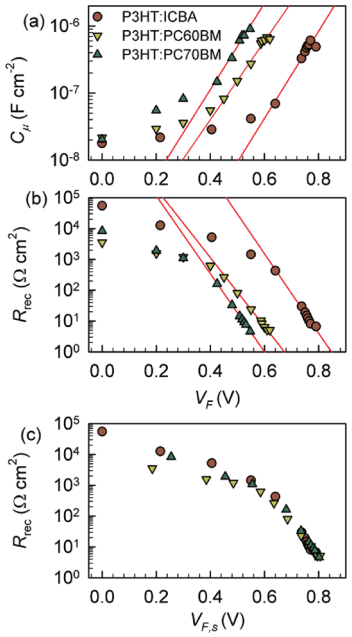

Figure 2. (a) Comparison of the chemical capacitance−voltage response of P3HT:fullerene-processed devices extracted from impedance analysis. Straight lines correspond to exponential fits as $C_\mu = C_0 \exp(\alpha q V_F/k_B T)$. (b) Recombination resistance R_{rec} as a function of the voltage. Straight lines correspond to exponential fits as $R_{rec} = R_0 \exp(-q\beta V_F/k_B T)$. (c) Same data as in panel b after applying a voltage shift extracted from the capacitance curves offset in panel a.

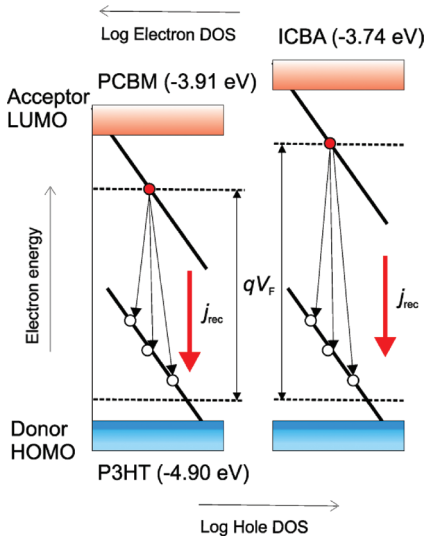

Figure 3. Diagram of the recombination mechanism proposed. Fullerene ICBA and PCBM bandgap DOS exhibit similar exponential distribution shifted with respect to the acceptor LUMO level. Recombining electron and holes are located in bandgap states, and the recombination charge transfer process takes place through fullerene electrons and polymer holes of different energies along the DOS. The output voltage V_F is originated by the Fermi level (dashed horizontal lines) splitting. The same recombination flux j_{rec} occurs for similar DOS occupancy as derived from a energy-independent recombination coefficient.

density p_0 that confers a semiconducting character (p-doping) to the donor material. Capacitance analysis (Mott−Schottky) plots are presented as Supporting Information, and it results in background hole densities $p_0 \sim 10^{15}$ cm^{-3}, as listed in Table 1.

Figure 2 shows that for larger voltages, the chemical capacitance exhibits the expected variation on voltage originated by the carrier occupation of electronic DOS as $C_\mu = q^2 L g(V_F)$,[20] where $g(E)$ is the DOS function and L is the active layer thickness. The DOS occupancy (identified from the exponential rise in the chemical capacitance) is shifted in energy depending on the fullerene LUMO position with respect to the donor HOMO level, as drawn in Figure 3 which compares P3HT:PCBM and P3HT:ICBA energetics. It is observed that C_μ exhibits an exponential dependence at high voltages, i.e., $C_\mu = C_0 \exp(\alpha q V_F/k_B T)$ with $\alpha \sim 0.35$ (see Table 1). C_μ extracted from the impedance analysis is then a replica of the bandgap electronic state distribution as the occupation progresses following the Fermi level displacement. It is important to note here that the presence of a hole background density makes the hole Fermi level modulation less sensible to the introduction of excess extra holes. For instance, if injected or photogenerated holes Δp equal the amount of background carriers, one would expect a Fermi level downward shift approximately equal to $\Delta E_{Fp} \approx k_B T \ln p_0/(\Delta p + p_0) = -17$ meV. This allows interpreting E_{Fp} as an energy reference that undergoes minor changes during photovoltaic operation. Instead, since the electron carriers density in equilibrium is negligible, the electron Fermi level E_{Fn} explores a significant portion of the electron DOS when excess carriers are injected or photogenerated, giving rise to the measured chemical capacitance.[21]

We have previously suggested[16] that recombination losses restrict the electronic site occupancy to lower-laying states of the DOS because surviving photogenerated carriers thermalize into the deepest levels available. Exponential[7] as well as Gaussian[16] DOS have been proposed accounting for the electron states distribution, although it is hard to distinguish between both of them in practical experiments because usual illumination intensities are only able to reach low-occupancy conditions (10^{14}−10^{17} cm^{-3}). Interestingly, the case of full occupation of intermediate electronic bands has been recently reported.[9]

The differential resistance R_{rec} extracted from impedance conveys information about the recombination flux. We have recently observed that P3HT-based solar cells operate under the electronic reciprocity relationship.[22] Under this principle, the voltage (Fermi level splitting) V_F fixes the local charge density, and the solar cell operation is viewed as a balance between voltage-independent photocurrent and illumination-

dx.doi.org/10.1021/jz3003958 | J. Phys. Chem. Lett. 2012, 3, 1386−1392

independent recombination current.[23] Recombination current is phenomenologically modeled as

$$j_{rec} = j_0 \exp\left(\beta \frac{qV_F}{k_B T}\right) \quad (2)$$

The expression in eq 2 for the recombination current is usually labeled as the β-recombination model that includes the parameter β accounting for the deviation from the diode ideal equation (inverse of the diode ideality factor).[24] Recombination resistance is defined from the recombination current derivative[16]

$$R_{rec} = \left(\frac{dj_{rec}}{dV_F}\right)^{-1} \quad (3)$$

Figure 2b shows that the recombination resistance corresponds to an approximate exponential behavior $R_{rec} = R_0 \exp(-\beta q V_F/k_B T)$ as expected from the derivative of eq 2. A straightforward estimation is obtained that results in $\beta \sim 0.70$ (see Table 1). At lower voltages R_{rec} tends to saturate presumably because the differential resistance measured is not only determined by the recombination flux but also by a shunt resistance caused by additional parallel leakage currents.

It is observed in Figure 2 that both parameters accounting for the recombination mechanisms (represented by R_{rec}), and the excess carrier accumulation (derived from C_μ), show a voltage dependence that approximately correlates with the difference in acceptor LUMO among different fullerene derivatives. As observed, PCBM-based devices produce similar $V_{oc} \approx 0.6$ V, in contrast to cells processed from ICBA ($V_{oc} \approx 0.8$ V). If the voltage offset between capacitance curves in Figure 2a is applied to compensate the shift in R_{rec}, we obtain the important result drawn in Figure 2c: a collapse in the recombination resistance appears, which directly suggests the occurrence of an energy-independent recombination loss kinetics.

With the aim to further explore these last findings, we discuss a more detailed view of the recombination mechanisms. In our approach, the recombination current is modeled as caused by charge transfer events among electrons and holes occupying fullerene and polymer bandgap states (Figure 3). Here we do *not* assume that recombination is mediated by prior capture from an extended state (conduction or valence band); instead, for simplicity reasons we assume the *direct* transfer from the localized DOS of electrons to that of holes, as noted in Figure 3. The recombination current can be formulated by considering electron and hole DOS, $g_n(E_n)$ and $g_p(E_p)$ (where E_n and E_p represents energy axis for electrons and holes, respectively), and the Fermi statistics, $f(E_F, E) = [1 + \exp(E - E_F/k_B T)]^{-1}$, as follows:[7]

$$j_{rec}(E_{Fn}, E_{Fp}) = qL \int_{-\infty}^{+\infty} \int_{-\infty}^{+\infty} g_n(E_n) f(E_{Fn}, E_n) g_p(E_p) [1 - f(E_{Fp}, E_p)] \nu_{rec}(E_n, E_p)\, dE_n\, dE_p \quad (4)$$

The structure of recombination model in eq 4 is as follows: all electron occupied states (in fullerene) are able to transfer to all hole-occupied (electron vacant) states in polymer, with a probability $\nu_{rec}(E_n, E_p)$ dependent on the energies E_n and E_p of the recombining electron and hole pair. Some remarks should be added. The first is that this model obviously disregards the spatial distribution of the carriers, in particular their distance to the interface. This assumption must be taken as a first-order approximation related to the fact that impedance spectroscopy and related macroscopic measurements just measure an *average Fermi* level and cannot resolve such microscopic details. So the model should resolve *energies* to a certain extent but averages over positions. In addition, in dynamical terms, one can describe more complex recombination mechanisms that involve carriers in different kinds of traps, or a combination of extended and localized states.[25,26] Different models involving total or trapped charge will lead to various interpretations of the parameter β. We have discussed the properties of the basic model of eq 4 in recent publications.[8,27] We have shown, in summary, that the simple assumptions giving rise to the current flux in eq 4 are able to generate the usually observed phenomenology: the V_{oc} loss with respect to the internal interface gap, the photovoltage temperature coefficient, and the temperature- and light intensity-dependence of the photocurrent. We have also shown that the separate chemical capacitances of electrons and holes are connected in series.[16]

If one further assumes as a first approximation that the recombination rate is only slightly energy dependent, i.e., $\nu_{rec}(E_n, E_p) = k$ is constant as inferred from the collapse of R_{rec} curves in Figure 2c, then eq 4 is simplified by decoupling the integration over the whole electron and hole DOS. This allows writing the recombination current as

$$j_{rec} = qLk\Delta n(\Delta p + p_0) \quad (5)$$

where k represents an energy-independent recombination coefficient, and the excess electron Δn and hole Δp densities appear in addition to background hole density p_0. Equation 5 has two limiting approximations: when $\Delta p \gg p_0$, the case of excess carriers greatly exceeding the background hole density, it is obtained that $j_{rec} \propto \Delta n^2$ because electroneutrality is obeyed ($\Delta n = \Delta p$). On the contrary, if $\Delta p \ll p_0$ one can infer that $j_{rec} \propto \Delta n$. The change of the recombination current dependence on the excess charge density is viewed as a transition between monomolecular (low Δn at lower voltages) to bimolecular (high Δn) mechanisms, as recently suggested using alternative methods.[28,29]

As stated previously, the impedance technique is able to separate parameters related to excess charge accumulation C_μ from recombination flux R_{rec}. This allows us to estimate the *excess* charge density Δn involved in the photovoltaic operation by integration as

$$\Delta n = \frac{1}{qL} \int_0^{V_F} C_\mu(V)\, dV \quad (6)$$

By applying eq 6, we obtain that the solar cell devices are able to accumulate $\Delta n \approx 3 \times 10^{16}$ cm^{-3} at voltages approaching V_{oc}. From eqs 2 and 3 it is derived that the recombination current can be written in terms of the recombination resistance as $j_{rec} = Lk_B T/\beta q R_{rec}$,[23] which allows for a straightforward calculation of the recombination coefficient k based on differential resistive and capacitive parameters extracted from impedance spectroscopy. By combining eqs 5 and 2 one arrives at

$$k = \frac{k_B T}{q^2 \Delta n(\Delta p + p_0)\beta R_{rec}} \quad (7)$$

The derivation of eq 7 assumes a nearly constant value for the recombination coefficient, independent of energetics of the states taking part on the recombination event. Results of applying eq 7 under the assumption of overall electroneutrality ($\Delta n = \Delta p$ and p_0 is compensated by immobile acceptor

dx.doi.org/10.1021/jz3003958 | J. Phys. Chem. Lett. 2012, 3, 1386−1392

dopants) are shown in Figure 4. It is observed that for $V_F > 0.4$ V, the recombination coefficient does exhibit an almost

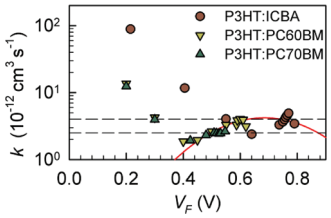

Figure 4. Recombination coefficient k calculated by means of eq 7 using the parameters extracted from the impedance analysis. Horizontal dashed lines mark the limits between 2.5−4.0 × 10^{-12} cm^3 s^{-1}. Solid line corresponds to the fitting of Marcus-like recombination coefficient (eq 8) to all data points. Reorganization energy $\lambda \sim 0.7$ eV accounts for the almost constant k because the charge transfer events occur near the maximum rate.

constant behavior within the order of $k \approx 10^{-12}$ cm^3 s^{-1}. A small increment is found for $PC_{60}BM$ fullerene between 2−4 × 10^{-12} cm^3 s^{-1}, in good agreement with previous reports.[7] In the case of P3HT:$PC_{70}BM$ devices, the same trend is encountered but with a minor variation (k = 2−3 × 10^{-12} cm^3 s^{-1}). P3HT:ICBA solar cells exhibit a bit larger values ($k \approx$ 4−6 × 10^{-12} cm^3 s^{-1}). For lower voltages, k departs from the approximate constant value because both R_{rec} and C_μ largely deviate from the exponential behavior. Hence points for voltages $V_F < 0.4$ V deviate from the constant trend because the capacitance value used in the calculation is not connected to the DOS occupancy (chemical capacitance), but to the depletion layer capacitance.

These findings are then a strong indication that the recombination kinetics depends weakly on the absolute energetics of the acceptor LUMO levels (fullerene electron affinity values). Moreover, results in Figure 4 point to the fact that the energy location of recombining carriers within the DOS has a minor influence on the recombination coefficient value. This validates our initial assumption (energy-independent k) used in deriving eq 5.

Validation of the bimolecular recombination law in eq 5 in the limiting case of high injection $\Delta p \gg p_0$ (valid for voltages approaching V_{oc} at 1 sun) can be reinforced from the experimental relationship between α and β parameters. The occupancy of bandgap states is modulated by α, which accounts for the characteristic energy of the DOS $\alpha = T/T_0$, with T_0 being the characteristic temperature of the exponential distribution $g(E) \propto \exp(E/k_BT_0) \propto \exp(\alpha E/k_BT)$. The energy E is identified with the voltage qV_F as explained previously (the chemical capacitance measures the DOS at the Fermi level). From eq 5 one can derive that the voltage-dependence of the recombination current is related to the exponential variation of the charge density as $j_{rec} \propto \Delta n^2 \propto \exp(2\alpha qV_F/k_BT)$. Comparing this last expression with eq 2, it is derived that $\beta = 2\alpha$. This last relationship corroborates our assumption of the same kind of carriers participating both in the DOS occupancy, and the recombination flux. As listed in Table 1, this last correlation is approximately obeyed. The parameter β, which shapes the recombination current in eq 2, is directly related to the profile of the $j-V$ curve, and consequently to the fill factor (FF).[20,30] It is therefore derived that energy disorder resulting in localization of charge carriers into bandgap states (extracted from C_μ) not only reduces the achievable V_{oc} as suggested in previous work,[8] but also has a detrimental effect on the reached FF through the modulation of the recombination current-dependence on voltage. The diode ideality factor encountered $1/\beta \approx 1.4$, along with the effect of the series resistance, are responsible for the low values extracted for FF ≈ 0.6.

The main finding extracted from our experiments is the independence of the carrier recombination kinetics on the donor HOMO/acceptor LUMO energy offset. This is an important result that puts severe constraints on the underlying charge transfer process accounting for recombination losses. As schematically drawn in Figure 3, recombination is viewed as a charge transfer event between reduced fullerene molecules and oxidized polymer chains. Recent TAS experiments performed with different fullerene dispersions in a P3HT matrix revealed that recombination kinetics is highly acceptor-independent at room-temperature.[31] Thermal motion inhibits the shielding effect of fullerene side groups observed at low temperatures, which points to a direct relationship between the effective distance between the polymer and the core fullerene, and the recombination kinetics. It is also well-known that charged organic molecules and polymers exhibit a strong electron−lattice coupling (polaronic states) that causes a significant distortion to the geometrical structure. Photoexcitation experiments found energy shifts caused by polaronic interaction of several hundreds of millielectronvolts.[32] After the reaction takes place, conformational distortions produced by the polaron interaction relax, restoring the molecular uncharged configuration. From the point of view of the Marcus theory for molecular reactions, the recombination event is expected to be accompanied by large reorganization energies λ because of the simultaneous polymer and fullerene structural relaxation.[33] The charge transfer rate k_0 in the semiclassical expression is written as

$$k_0 = \frac{2\pi}{\hbar} |V_{if}|^2 \sqrt{\frac{1}{4\pi\lambda k_B T}} \exp\left(-\frac{(\Delta G_0 + \lambda)^2}{4\lambda k_B T}\right) \quad (8)$$

where, ΔG_0 is the variation of the Gibbs free energy during the reaction, and V_{if} corresponds to the electronic coupling matrix element. We identify here ΔG_0 with the acceptor and donor energy offset, $\Delta G_0 \sim E_n - E_p$. The fact that the charge transfer reaction kinetics (as inferred from the almost constant $k \approx 10^{-12}$ cm^3 s^{-1} found) is not altered by the energy offset would then suggest a relatively large value of λ in such a way that the reaction occurs in the vicinity of the maximum rate. For large λ values, the charge transfer kinetics is less sensible to changes of the energy offset. This last speculation is checked by fitting a Marcus-like recombination coefficient, which follows the energy dependence introduced in eq 8 to all k data values. By means of this approach, we interpret Figure 4 as representing the Fermi level dependence of an effective recombination coefficient. As observed in Figure 4, the Marcus theory predicts a large value for the reorganization energy $\lambda \approx 0.7$ eV in accordance with the preceding arguments. It is found that both $PC_{60}BM$- and $PC_{70}BM$-based devices exhibit a small increment with the energy in good accordance with charge transfer events occurring within the normal Marcus region. For larger energies (higher ICBA LUMO levels), the recombination process takes place near the maximum flat region. Therefore it is the reorganization energy λ rather than the donor/acceptor energy offset that governs the kinetics of recombination for this kind of P3HT:fullerene device. We observe finally that recombination

dx.doi.org/10.1021/jz3003958 | J. Phys. Chem. Lett. 2012, 3, 1386−1392

mechanisms are directly connected to molecular characteristics, in good agreement with previous reports.[34]

In conclusion, a detailed analysis of the charge carrier recombination mechanism has been presented based on parameters extracted from impedance spectroscopy technique. Chemical capacitance values indicate the distribution of excess carriers within bandgap density-of-states. The recombination resistance corresponds to the derivative of the carrier recombination flux. The impedance technique allows extracting parameters related to energetics as well as recombination kinetics simultaneously. By using active layers blended with fullerene acceptors of different electron affinity, we have demonstrated that the recombination coefficient is only slightly dependent on the fullerene LUMO energy. Moreover, the energy location of recombining carriers within the DOS has also a minor influence on the recombination coefficient value, which results in values on the order of $k \approx 10^{-12}$ cm^3 s^{-1}. It is proposed that charge transfer events accounting for the recombination process take place in the vicinity of the maximum rate in the framework of the Marcus theory, with large reorganization energy values that govern recombination kinetics. We finally conclude that V_{oc} enhancement is exclusively caused by the larger donor HOMO/acceptor LUMO offset, because the carrier recombination process appears to be highly independent of the fullerene energetics.

EXPERIMENTAL SECTION

Device Fabrication. P3HT (Aldrich), ICBA (Luminescence Technology Corp.), $PC_{60}BM$ (Nano-C, 99.5%), $PC_{70}BM$ (Nano-C, 99%), PEDOT:PSS (CLEVIOS P AI 4083), o-dichlorobenzene (Aldrich, 99.9%), Ca (Aldrich, 99.995%), and silver (Aldrich,99.99%) were used as received without further purification. All manipulations were carried out in a glovebox under a nitrogen atmosphere unless otherwise stated. P3HT:fullerene blends were prepared in a 1:1 ratio from dry o-dichlorobenzene (17 mg/mL) and were stirred at room temperature. P3HT:$PC_{60}BM$ and P3HT:$PC_{70}BM$ blends were prepared 24 h prior to sample fabrication. P3HT:ICBA was mixed 2 h before sample preparation according to a previously reported procedure. Polymer solar cells were fabricated with a standard sandwich structure of ITO/PEDOT:PSS/P3HT:fullerene/Ca/Ag, and 9 mm^2 of active area. PEDOT:PSS was spin coated in air at 5500 rpm for 30 s onto an ITO-coated glass substrate (10 Ohm/sq), film thickness of ∼35 nm. The substrates were heated at 120 °C for 10 min to remove traces of water and were transferred to a glovebox equipped with a thermal evaporator. The P3HT:fullerene layer was deposited at speeds of 1200 rpm (thickness was about 110 nm) for 30 s followed by a slow drying of the film in a Petri dish. At this point, samples were thermally annealed at 130 °C for 20 min. Evaporation was carried out at a base pressure of 3×10^{-6} mbar and Ca (10 nm) and Ag (100 nm) were sequentially evaporated. Devices were encapsulated by using a pressure-sensitive glue (polyisobutylene, Oppanol B 12 SFN from BASF) and a glass microscopy slide. Samples were then taken out of the glovebox for device characterization.

Device Characterization. Current density−voltage and impedance measurements were carried out by illumination with a 1.5 G illumination source (1000 W m^{-2}) using an Abet Sun 2000 Solar Simulator. The light intensity was adjusted with a calibrated Si solar cell. For impedance measurements, different light intensities were achieved with wavelength-independent perforated metal attenuators, which moderate system output without spoiling its spatial or spectral uniform. Impedance spectra were recorded by applying a small voltage perturbation (20 mV rms) at frequencies from 1 MHz to 1 Hz. Measurements were carried out either under open circuit potential conditions by applying a bias voltage equal to V_{oc} at each light intensity, or in the dark at different bias voltage to extract the capacitance−voltage characteristics. These measurements were performed with Autolab PGSTAT-30 equipped with a frequency analyzer module. Recombination resistance R_{rec} and chemical capacitance C_μ were directly extracted from the low-frequency arc.

ASSOCIATED CONTENT

Supporting Information

Capacitance/voltage curves for the different devices. This material is available free of charge via the Internet http://pubs.acs.org.

AUTHOR INFORMATION

Corresponding Author

*E-mail: bisquert@uji.es, garciag@uji.es.

Notes

The authors declare no competing financial interest.

ACKNOWLEDGMENTS

We acknowledge financial support from the Ministerio de Economia y Competitividad under project HOPE CSD2007-00007 (Consolider-Ingenio 2010), and Generalitat Valenciana (Prometeo/2009/058, ACOMP/2009/056, ACOMP/2009/095, and ISIC/2012/008, Institute of Nanotechnologies for Clean Energies). L.F.M. acknowledges Conselho Nacional de Desenvolvimento Científico e Tecnológico (CNPq) for a grant (201380/2010-2).

REFERENCES

(1) Lenes, M.; Wetzelaer, G.-J. A. H.; Kooisrta, F. B.; Veenstra, S. C.; Hummelen, J. C.; Blom, P. W. M. Fullerene Bisadducts for Enhanced Open-Circuit Voltages and Efficiencies in Polymer Solar Cells. *Adv. Mater.* **2008**, *20*, 2116−2119.

(2) Ross, R. B.; Cardona, C. M.; Guldi, D. M.; Sankaranaravanan, S. G.; Reese, M. O.; Kopidakis, N.; Peet, J.; Walker, B.; Bazan, G. C.; Van Keuren, E.; Holloway, B. C.; Drees, M. Endohedral Fullerenes for Organic Photovoltaic Devices. *Nat. Mater.* **2009**, *8*, 208−212.

(3) He, Y.; Chen, H.-Y.; Hou, J.; Li, Y. Indene-C60 Bisadduct: A New Acceptor for High-Performance Polymer Solar Cells. *J. Am. Chem. Soc.* **2010**, *132*, 1377−1382.

(4) Zhao, G.; Hi, Y.; Li, Y. 6.5% Efficiency of Polymer Solar Cells Based on Poly(3-hexylthiophene) and Indene-C 60 Bisadduct by Device Optimization. *Adv. Mater.* **2010**, *22*, 4355−4358.

(5) Cheng, Y.-J.; Liao, M.-H.; Chang, C.-Y.; Kao, W.-S.; Wu, C.-E.; Hsu, C.-S. Di(4-mephylphenyl)mathano-C_{60} Bis-Adduct for Efficient and Stable Organic Photovoltaics with Enhanced Open-Circuit Voltage. *Chem. Mater.* **2011**, *23*, 4056−4062.

(6) Kim, H.; Seo, J. H.; Park, E. Y.; Kim, T.-D.; Lee, K.; Lee, K.-S.; Cho, S.; Heeger, A. J. Increased Open-Circuit Voltage in Bulk-Heterojunction Solar Cells Using a C_{60} Derivative. *Appl. Phys. Lett.* **2010**, *97*, 193309.

(7) Maurano, A.; Hamilton, R.; Shuttle, C. G.; Ballantyne, A. M.; Nelson, J.; O'Regan, B.; Zhang, W.; McCulloch, I.; Azimi, H.; Morana, M.; Brabec, C. J.; Durrant, J. R. Recombination Dynamics As a Key Determinant of Open Circuit Voltage in Organic Bulk Heterojunction Solar Cells: A Comparison of Four Different Donor Polymers. *Adv. Mater.* **2010**, *22*, 4987−4992.

(8) Garcia-Belmonte, G.; Bisquert, J. Open-Circuit Voltage Limit Caused by Recombination through Tail States in Bulk Heterojunction Polymer-Fullerene Solar Cells. *Appl. Phys. Lett.* **2010**, *96*, 113301.
(9) Garcia-Belmonte, G.; Boix, P. P.; Bisquert, J.; Lenes, M.; Bolink, H. J.; La Rosa, A.; Filippone, S.; Martín, N. Influence of the Intermediate Density-of-States Occupancy on Open-Circuit Voltage of Bulk Heterojunction Solar Cells with Different Fullerene Acceptors. *J. Phys. Chem. Lett.* **2010**, *1*, 2566−2571.
(10) Mozer, A. J.; Dennler, G.; Sariciftci, N. S.; Westerling, M.; Pivrikas, A.; Österbacka, R.; Juska, G. Time-Dependent Mobility and Recombination of the Photoinduced Charge Carriers in Conjugated Polymer/Fullerene Bulk Heterojunction Solar Cells. *Phys. Rev. B* **2005**, *72*, 035217.
(11) Pivrikas, A.; Juska, G.; Mozer, A. J.; Scharber, M.; Arlauskas, K.; Sariciftci, N. S.; Stubb, H.; Österbacka, R. Bimolecular Recombination Coefficient as a Sensitive Testing Parameter for Low-Mobility Solar-Cell Materials. *Phys. Rev. Lett.* **2005**, *94*, 176806.
(12) Juska, G.; Sliauzys, G.; Genevicius, K.; Arlauskas, K.; Pivrikas, A.; Scharber, M.; Dennler, G.; Sariciftci, N. S.; Österbacka, R. Charge-Carrier Transport and Recombination in Thin Insulating Films Studied via Extraction of Injected Plasma. *Phys. Rev. B* **2006**, *74*, 115314.
(13) Montanari, I.; Nogueira, A. F.; Nelson, J.; Durrant, J. R.; Winder, C.; Loi, M. A.; Sariciftci, N. S.; Brabec, C. Transient Optical Studies of Charge Recombination Dynamics in a Polymer/Fullerene Composite at Room Temperature. *Appl. Phys. Lett.* **2002**, *81*, 3001−3003.
(14) Arndt, C.; Zhokhavets, U.; Mohr, M.; Gobsch, G.; Al-Ibrahim, M.; Sensfuss, S. Determination of Polaron Lifetime and Mobility Polymer/Fullerene Solar Cells by Means of Photoinduced Absorption. *Synth. Met.* **2004**, *147*, 257−260.
(15) Shuttle, C. G.; O'Regan, B.; Ballantyne, A. M.; Nelson, J.; Bradley, D. D. C.; de Mello, J.; Durrant, J. R. Experimental Determination of the Rate Law for Charge Carrier Decay in a Polythiophene:Fullerene Solar Cell. *Appl. Phys. Lett.* **2008**, *92*, 093311.
(16) Garcia-Belmonte, G.; Boix, P. P.; Bisquert, J.; Sessolo, M.; Bolink, H. J. Simultaneous Determination of Carrier Lifetime and Electron Density-of-States in P3HT:PCBM Organic Solar Cells under Illumination by Impedance Spectroscopy. *Sol. Energy Mater. Sol. Cells* **2010**, *94*, 366−375.
(17) Foertig, A.; Baumann, A.; Rauh, D.; Dyakonov, V.; Deibel, C. Charge Carrier Concentration and Temperature Dependent Recombination in Polymer−Fullerene Solar Cells. *Appl. Phys. Lett.* **2009**, *95*, 052104.
(18) Boix, P. P.; Ajuria, J.; Pacios, R.; Garcia-Belmonte, G. Carrier Recombination Losses in Inverted Polymer:Fullerene Solar Cells with ZnO Hole-Blocking Layer from Transient Photovoltage and Impedance Spectroscopy Techniques. *J. Appl. Phys.* **2011**, *109*, 074514.
(19) Scharber, M.; Mühlbacher, D.; Koppe, M.; Denk, P.; Waldauf, C.; Heeger, A. J.; Brabec, C. J. Design Rules for Donor Bulk-Heterojunction Solar Cells-Towards 10% Energy-Conversion Efficiency. *Adv. Mater.* **2006**, *18*, 789−794.
(20) Fabregat-Santiago, F.; Garcia-Belmonte, G.; Mora-Seró, I.; Bisquert, J. Characterization of Nanostructured Hybrid and Organic Solar Cells by Impedance Spectroscopy. *Phys. Chem. Chem. Phys.* **2011**, *13*, 9083−9118.
(21) Bisquert, J.; Garcia-Belmonte, G. On Voltage, Photovoltage and Photocurrent in Bulk Heterojunction Organic Solar Cells. *J. Phys. Chem. Lett.* **2011**, *2*, 1950−1964.
(22) Donolato, C. A Reciprocity Theorem for Charge Collection. *Appl. Phys. Lett.* **1985**, *46*, 270−272.
(23) Boix, P. P.; Guerrero, A.; Marchesi, L. F.; Garcia-Belmonte, G.; Bisquert, J. Current-Voltage Characteristics of Bulk Heterojunction Organic Solar Cells: Connection Between Light and Dark Curves. *Adv. Energy Mater.* **2011**, *1*, 1073−1078.
(24) Bisquert, J.; Mora-Seró, I. Simulation of Steady-State Characteristics of Dye-Sensitized Solar Cells and the Interpretation of the Diffusion Length. *J. Phys. Chem. Lett.* **2010**, *1*, 450−456.
(25) Kirchartz, T.; Pieters, B. E.; Kirkpatrick, J.; Rau, U.; Nelson, J. Recombination via Tail States in Polythiophene:Fullerene Solar Cells. *Phys. Rev. B* **2011**, *83*, 115209.
(26) Street, R. A. Localized State Distribution and Its Effects on Recombination in Organic Solar Cells. *Phys. Rev. B* **2011**, *84*, 075208.
(27) Garcia-Belmonte, G. Temperature Dependence of Open-Circuit Voltage in Organic Solar Cells from Generation−Recombination Kinetic Balance. *Sol. Energy Mater. Sol. Cells* **2010**, *94*, 2166−2169.
(28) Leong, W. L.; Cowan, S. R.; Heeger, A. J. Differential Resistance Analysis of Charge Carrier Losses in Organic Bulk Heterojunction Solar Cells: Observing the Transition from Bimolecular to Trap-Assisted Recombination and Quantifying the Order of Recombination. *Adv. Energy Mater.* **2011**, *1*, 517−522.
(29) Thakur, A. K.; Wantz, G.; Garcia-Belmonte, G.; Bisquert, J.; Hirsch, L. Temperature Dependence of Open-Circuit Voltage and Recombination Processes in Polymer−Fullerene Based Solar Cells. *Sol. Energy Mater. Sol. Cells* **2011**, *95*, 2131−2135.
(30) Green, M. A. *Solar Cells: Operating Principles, Technology, and System Applications*; Prentice Hall: Upper Saddle River, NJ, 1981.
(31) Busby, E.; Rochester, C. W.; Moulé, A. J.; Larsen, D. S. Acceptor Dependent Polaron Recombination Dynamics in Poly-3-hexylthiophene:Fullerene Composite Films. *Chem. Phys. Lett.* **2011**, *513*, 77−83.
(32) Jiang, X. M.; Österbacka, R.; Korovyanko, O.; An, C. P.; Horovitz, B.; Janssen, R. A. J.; Vardeny, Z. V. Spectroscopic Studies of Photoexcitations in Regioregular and Regiorandom Polythiophene Films. *Adv. Funct. Mater.* **2002**, *12*, 587−597.
(33) Marcus, R. A. Electron Transfer Reactions in Chemistry. Theory and Experiment. *Rev. Mod. Phys.* **1993**, *65*, 599−610.
(34) Schlenker, C. W.; Thompson, M. E. The Molecular Nature of Photovoltage Losses in Organic Solar Cells. *Chem. Commun.* **2011**, *47*, 3702−3716.